ISSN (Print) 1226-1750
ISSN (Online) 2233-6656
Journal of Magnetics 27(2), 186-200 (2022) https://doi.org/10.4283/JMAG.2022.27.2.186

A Report of Generalized Blood Flow Model with Heat Conduction Between Blood and Particles

Farhad Ali[1]*, Fazli Haq[1], Naveed Khan[1], Hessah Alqahtani[2], Anees Imtiaz[1], and Ilyas Khan[3]

[1]*Department of Mathematics, City University of Science and Information Technology, Peshawar, 25000, Pakistan*
[2]*Department of Mathematics, Faculty of Science and Arts, King Abdulaziz University, Rabigh, Saudi Arabia*
[3]*Department of Mathematics, College of Science Al-Zulfi, Majmaah University, Al-Majmaah 11952, Saudi Arabia*

(Received 12 February 2022, Received in final form 26 March 2022, Accepted 26 March 2022)

This paper examines the magneto hydrodynamic two-phase blood (Casson fluid) flow in a vessel with heat conduction between blood and particles. The temperature of both phases is also considered. The model for the flow under consideration is formulated in terms of partial differential equations. Then the classical model is generalized by utilizing the Caputo fractional order derivative. The generalized equations are then non-dimensionalized by using appropriate dimensionless variables. The exact dimensionless solutions are obtained via the joint application of Laplace & Hankel integral transforms. The influence of various embedded parameters on both the velocities (blood and magnetic particles) and the temperature distribution are presented graphically. It is worth noting that the particle and blood velocities decrease for increasing the values of magnetic parameter (*H*) which is useful to control the blood flow during magnetic therapy (for treating pain, such as the back, foot, or joint pain) and surgeries. It is worth noting that fractional model better describes the flow behavior than classical model by providing virous integral curves as shown in Fig.

Keywords : Casson fluid, two-phase blood flow, heat conduction, magneto hydrodynamic, Caputo fractional order derivative, Laplace & Hankel integral transforms

1. Introduction

Bio magnetic fluid dynamics (BFD) is the new research area in fluid dynamics that studies the bio fluids flow in the presence of a magnetic field. In medical sciences and bioengineering, bio magnetic fluid dynamics have several applications, specifically in targeting drug delivery [1]. It reduces blood loss in the process of surgeries and cures cancer tumors via hyperthermia [2]. It can also be applied to improve magnetic devices for the separation of cells [3]. In BFD the most suitable fluid is blood. Blood is the suspension of RBC's or erythrocytes and plasma (watery fluid) [4]. Because of the presence of erythrocytes, blood behaves like a bio magnetic fluid. Erythrocytes are the red blood cells that contain hemoglobin which plays the role of magnetic particles and carrying oxygen to the body. Due to the negative charge, erythrocytes create a magnetic field on the walls of the vessel. Usually, targeted drug delivery is used to magnetize the blood by adding nanoparticles. The first bio magnetic fluid model was suggested by Haik *et al.* [5]. They studied the models for ferrohydrodynamics (FHD) and BFD comparatively and assumed that the flow is under the magnetic field's impact, but the induced magnetic field is not considered. Blood is an example of Casson fluid defined as the shear thinning liquids and is accepted to have an infinite viscosity at zero deformation [6]. When the yield stress is applied to fluids, and the shear stresses less than the yield stresses, the fluids behave like a solid. However, when the shear stresses are larger than the yield stress applied, it begins to flow. The flow of blood with larger shear rates through arteries of large diameter shows Newtonian behavior, but blood flow with low rate of shear through small arteries shows non-Newtonian behavior [7, 8]. The flow of blood with a low shear rate through narrow arteries shows a Casson fluid [9-11]. The mathematical model for the flow of blood through narrow arteries with low shear rates has been presented by many researchers [12-14]. For narrow capillaries of diameter 130 μm-1000 μm, the Casson fluid model is appropriate and discussed

*Corresponding author: Tel: +92-03328882933
Fax: +92-03328882933, e-mail: farhadali@cusit.edu.pk

by Chamkha *et al*. [15, 16].

The heat transfer can be noticed in various fields of industry. It has many applications in the gas and oil industry, chemical industry, and pharmaceutical industry. Radiation, conduction, and convection are the three different modes in which heat transfers [17]. The transfer of heat in the form of gas or liquid to colder matter from warmed matter is called convection [18]. The uses of heat transmission are established in electrical devices, thermal power stations engineering, automotive engineering, insulation, and climate control [19]. The unsteady Casson fluid flow and heat transfer over a moving flat plate is considered by Mustafa *et al.* [20]. Hayat *et al.* [21] found the solutions using the Homotopy analysis method to discuss the Casson fluid in stretching cylinder with nanoparticles and thermal radiations. In the above study, the researchers studied the classical Casson fluid models. The classical derivatives were use, and fractional-order derivatives were ignored because of their complexities [19-21].

Fractional calculus is the generalization of ordinary calculus in which the non-integer order derivative and integrals have been discussed. Fractional calculus was developed three hundred years ago by Laplace, Fourier, Abel, and Liouville [22]. Fractional calculus is applied in science, biosciences, mathematics, electrochemistry, physics, engineering, and technology [23]. Moreover, fractional derivatives have several applications in fluid mechanics, mathematical biology, viscoelasticity, electrochemistry, and signal processing [24-28]. Therefore, the significance of fractional order derivatives cannot be ignored. Bakhti *et al.* [29] considered the pulsatile flow of blood through stenosed arteries because of pressure gradient using fractional-order derivatives. Ali *et al.* [30] examined blood flow as a Casson fluid through a horizontal tube and considering the fractional-order derivative. Shah *al.* [31] considered the fractional-order derivative to investigate the flow of blood with magnetic particles and obtained the solutions by the joint use of Laplace & Hankel transformations. Imran *et al.* [32] studied the differential type fluid with mass and heat transfer by considering the Caputo derivatives. For blood flow in the presence of a magnetic field due to periodic pressure gradient inside the oscillatory arteries, a fractional order model is proposed by Bansi *et al.* [33].

This article aims to study the impact of magnetic field on blood flow to discuss the importance and role of magnetic field in different areas of biomedicine. In drug delivery, magnetically guided drug targeting has been used in order to enhance the efficacy and reduce the unpleasant side effects associated with chemotherapy. This method of drug delivery involves immobilization of drug or radionuclide in biocompatible magnetic nano- or microspheres. This method of delivery makes chemotherapy more effective by increasing the drug concentration at the tumour site while limiting the systemic drug concentration. The magnetic particles are used to deliver a package, such as an anticancer drug, or a cohort of radionuclide atoms, to a targeted region of the body, such as a tumour. Magnetic therapy can be very useful to the conditions like headaches, travel sickness, poor circulation, muscles sprains, strains and joints pain. In the above literature, so far no one has considered the Casson fluid model for blood flow with heat conduction between blood and particles with fractional derivatives. In this paper, the blood as a fractional Casson fluid flow in the presence of a magnetic field and heat conduction between the particles and blood through a vessel studied. Exact solutions for both the velocities (blood and particle) and both the temperatures (blood and particles) are obtained via the Laplace & Hankel transforms. The influence of different parameters on the blood flow, particles velocity, temperature of blood and particles is graphically studied.

2. Mathematical Formulation

In this paper, the non-Newtonian flow of blood with a magnetic particle is studied in a vessel of radius R_0 as shown in Fig. 1. We assume that the magnetic particles are equally dispersed in the blood. The vessel is taken along the z-axis, and the radial axis is r. The magnetic field acts perpendicularly on the flow direction. Because of the smallness of the magnetic Reynolds number (Re), the induced magnetic field is neglected [34]. At the time $t = 0$, the vessel, particles, and blood are assumed to be at rest.

Under the impact of a transverse applied magnetic field,

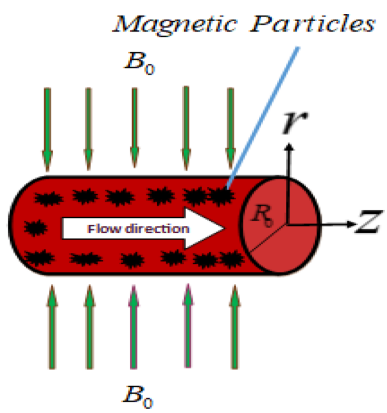

Fig. 1. (Color online) Schematic representation of the flow model.

the equation of blood velocity in a vessel is given by [35, 36]:

$$\frac{\partial w(r,t)}{\partial t} = -\frac{1}{\rho}\frac{\partial p}{\partial z} + \frac{\mu}{\rho}\left(1+\frac{1}{\beta}\right)\left\{\frac{\partial^2 w(r,t)}{\partial r^2} + \frac{1}{r}\frac{\partial w(r,t)}{\partial r}\right\} + \frac{KN}{\rho}\left\{w_1(r,t) - w(r,t)\right\} - \frac{\sigma B^2{}_0}{\rho} w(r,t). \tag{1}$$

The oscillatory pressure gradient $\frac{\partial p}{\partial z}$ is given as [37]:

$$-\frac{\partial p}{\partial z} = b_0 + b_1\cos(\omega t), \qquad t > 0. \tag{2}$$

Where w is the velocity of blood, w_1 is the particle velocity, ρ is the density of blood, μ is the dynamic viscosity, $\beta = \frac{\mu_B\sqrt{2\pi_c}}{\tau_r}$ is the parameter for Casson fluid in which μ_B, τ_r & π_c are the plastic dynamic viscosity, yield stress and the critical value of this product based on a non-Newtonian fluid model respectively. The third term on the right-hand side of Eq. (1). i.e $\frac{KN}{\rho}\left(w_1(r,t) - w(r,t)\right)$ shows the forces between blood and magnetic particles because of the relative motion. Where K & N are the Stokes constant, and the number of magnetic particles per unit volume, σ is the electrical conductivity, B_0 is the applied magnetic field, b_0 is the systolic and b_1 is the diastolic amplitudes of pressure gradient and ω is the frequency [38, 39].

From Newton's 2nd law, the governing equation of particles (magnetic) is given in the form [40]:

$$m\frac{\partial w_1}{\partial t} = K\left\{w(r,t) - w_1(r,t)\right\}. \tag{3}$$

Where m, and w_1 are the mass and velocity of particles, respectively.

The temperature equation of the blood is given by [41, 42]:

$$\frac{\partial T(r,t)}{\partial t} = \frac{k}{\rho C_p}\left(\frac{\partial^2 T(r,t)}{\partial r^2} + \frac{1}{r}\frac{\partial T(r,t)}{\partial r}\right) - \frac{4\zeta^2}{\rho C_p}(T - T_\infty) + \frac{\mu}{\rho C_p}\left(\frac{\partial w}{\partial r}\right)^2 + \frac{\rho_s C_s}{\rho C_p \gamma_T}(T_s - T), \tag{4}$$

where T represents the blood temperature, k and C_p, represent the thermal conductivity and specific heat at constant pressure respectively, ζ^2 is the Planck mean linear absorption coefficient, $\left(\frac{\partial w}{\partial r}\right)^2$ represents the viscous dissipation, ρ_s and C_s represent the density and specific heat of particles respectively, γ_T is the temperature relaxation time parameter and T_s is the temperature of particles.

The temperature equation of particles is given by [43]:

$$\frac{\partial T_s(r,t)}{\partial t} = \frac{1}{\gamma_T}\left(T - T_s\right), \qquad t > 0,\ r \in \left(0,\ R_0\right). \tag{5}$$

The corresponding initial conditions and boundary conditions are given by:

$$\left.\begin{array}{l} w(r,0) = 0, \quad w_1(r,0) = 0 \\ w(R_0,t) = 0, \quad w_1(R_0,t) = 0 \\ T(r,\ 0) = T_\infty,\ T(R_0,\ t) = T_w \\ T_s(r,0) = T_\infty,\ T_s(R_0,t) = T_w \\ \left.\frac{\partial w(r,t)}{\partial r}\right|_{r=0} = 0 \end{array}\right]. \tag{6}$$

Multiplying each term of Eqs. (1), (3), (4), and (5) by $\lambda = \sqrt{\frac{R_0\rho}{b_0}}$ to convert from their classical derivative to the Caputo fractional derivative

$$\lambda^\alpha D_t^\alpha w(r,t) = \frac{\lambda}{\rho}\left[b_0 + b_1\cos(\omega t)\right] + \lambda\nu\left(1+\frac{1}{\beta}\right)\left\{\frac{\partial^2 w(r,t)}{\partial r^2} + \frac{1}{r}\frac{\partial w(r,t)}{\partial r}\right\} + \lambda\frac{KN}{\rho}\left\{w_1(r,t) - w(r,t)\right\} - \frac{\lambda\sigma B^2{}_0}{\rho} w(r,t), \tag{7}$$

$$\lambda^\alpha D_t^\alpha w_1(r,t) = \frac{\lambda K}{m}\left\{w(r,\ t) - w_1(r,\ t)\right\}, \tag{8}$$

$$\lambda^\alpha D_t^\alpha T(r,t) = \frac{k\lambda}{\rho C_p}\left\{\frac{\partial^2 T(r,t)}{\partial r^2} + \frac{1}{r}\frac{\partial T(r,t)}{\partial r}\right\} - \frac{4\lambda\zeta^2}{\rho C_p}(T - T_\infty) + \frac{\lambda\nu}{C_p}\left(\frac{\partial w}{\partial r}\right)^2 + \frac{\lambda\rho_s C_s}{\rho C_p \gamma_T}(T_s - T), \tag{9}$$

$$\lambda^\alpha D_t^\alpha T_s(r,t) = \frac{\lambda}{\gamma_T}\left(T - T_s\right), \tag{10}$$

where;

$$D_t^\alpha f(r,t) = \frac{1}{\Gamma(1-\alpha)}\int_0^t \frac{1}{(t-\tau)^\alpha}\frac{\partial f(r,\tau)}{\partial \tau}d\tau, \tag{11}$$

is the Caputo time derivative of fractional order α [44]:

By introducing the appropriate non dimensional variables:

$$r^* = \frac{r}{R_0},\ t^* = \frac{t}{\lambda},\ w^* = \frac{w}{u_0},\ w_1^* = \frac{w_1}{u_0},\ b_0^* = \frac{\lambda b_0}{\rho u_0},\ b_1^* = \frac{\lambda b_1}{\rho u_0},\ \omega^* = \lambda\omega,$$
$$T^* = \frac{T - T_\infty}{T_w - T_\infty},\ T_s = \frac{T_s - T_\infty}{T_w - T_\infty}. \tag{12}$$

After introducing the dimensionless variables and

dropping the (*) notation Eqs. (7-10), take the form

$$D_t^{\alpha} w(r,t) = [b_0 + b_1 \cos(\omega t)] + \beta_1 \frac{\partial^2 w(r,t)}{\partial r^2} + \frac{\beta_1}{r}\frac{\partial w(r,t)}{\partial r} + R\{w_1(r,t) - w(r,t)\} - Hw(r,t). \quad (13)$$

$$GD_t^{\alpha} w_1(r,t) = \{w(r,t) - w_1(r,t)\}. \quad (14)$$

$$P_e D_t^{\alpha} T(r,t) = \left(\frac{\partial^2 T(r,t)}{\partial r^2} + \frac{1}{r}\frac{\partial T(r,t)}{\partial r}\right) - 4R_a T(r,t) + B_r\left(\frac{\partial w}{\partial r}\right)^2 + R_s(T_s(r,t) - T(r,t)). \quad (15)$$

$$D_t^{\alpha} T_s(r,t) = \gamma\,(T - T_s). \quad (16)$$

$$\beta_1 = \frac{1}{\mathrm{Re}}(1+\frac{1}{\beta}),\ \mathrm{Re} = \frac{R_0^{\ 2}}{\lambda\nu},\ R = \frac{\lambda KN}{\rho},\ H = \sqrt{\frac{\lambda\sigma B_0^{\ 2}}{\rho}},$$

$$G = \frac{m}{K\lambda},\ P_e = \frac{\rho C_p R_0^{\ 2}}{k\lambda},\ R_a = \frac{\alpha^2 R_0^{\ 2}}{k},\ B_r = \frac{\mu u_0^{\ 2}}{k(T_w - T_\infty)},$$

$$R_s = \frac{\rho_s C_s R_0^{\ 2}}{k\gamma_T} \text{ and } \gamma = \frac{\lambda}{\gamma_T}.$$

Where Re is the Reynold number, R is the concentration parameter of particle, H^2 is the magnetic parameter, G is the parameter for particle mass. P_e, and R_a show the Peclet number and radiation absorption parameter respectively. B_r, and R_s represent the Brinkman number and particle concentration parameter, and γ is the temperature relaxation time-parameter.

The initial & boundary conditions become:

$$\left.\begin{array}{ll} w(r,0)=0, & w_1(r,0)=0 \\ w(1,t)=0, & w_1(1,t)=0 \\ T(r,0)=0, & T(1,t)=1 \\ T_s(r,0)=0, & T_s(1,t)=1 \\ & \left.\dfrac{\partial w}{\partial r}\right|_{r=0}=0 \end{array}\right\}. \quad (17)$$

3. Solution of the Problem

To find the solution to the problem, we use the Laplace and Hankel transforms jointly.

3.1. Solution of Velocity Equation

By applying the Laplace transform to Eq. (13) and Eq. (14), respectively, and using the initial conditions, we get:

$$s^{\alpha}\overline{w}(r,s) = \frac{b_0}{s} + b_1\frac{s}{s^2+\omega} + \beta_1\left(\frac{\partial^2\overline{w}(r,s)}{\partial r^2} + \frac{1}{r}\frac{\partial\overline{w}(r,s)}{\partial r}\right) + R\overline{w_1}(r,s) - \overline{w}(r,s)(R+H), \quad (18)$$

$$\overline{w_1}(r,s) = \frac{\overline{w}(r,s)}{Gs^{\alpha}+1}. \quad (19)$$

With the boundary conditions in the transformed form:

$$\overline{w}(1,s) = 0,\quad \overline{w_1}(1,s) = 0. \quad (20)$$

Using Eq. (19) into Eq. (18), we get:

$$s^{\alpha}\overline{w}(r,s) = \frac{b_0}{s} + b_1\frac{s}{s^2+\omega^2} + \beta_1\left(\frac{\partial^2\overline{w}(r,s)}{\partial r^2} + \frac{1}{r}\frac{\partial\overline{w}(r,s)}{\partial r}\right) + R\left(\frac{\overline{w}(r,s)}{Gs^{\alpha}+1}\right) - \overline{w}(r,s)(R+H), \quad (21)$$

by using the finite Hankel transform of zero-order [45, 46] in Eq. (21) and applying the boundary conditions from Eq. (20), we get:

$$\overline{w}_H(r_n,s)\left[\frac{Gs^{2\alpha} + \{1 + G(R+H^2) + \beta_1 r_n^{\ 2} + H\}}{Gs^{s\alpha}+1}\right] = \left(\frac{b_0}{s} + b_1\frac{s}{s^2+\omega^2}\right)\frac{J_1(r_n)}{r_n}. \quad (22)$$

Where $\overline{w}_H(r_n,s) = \int_0^1 r\overline{w}(r_n,s)J_0(rr_n)dr$ is the finite Hankel transform of zero-order of $\overline{w}(r,s)$, and r_n (n = 1,2,3,4,...) are the positive roots of $J_0(x)=0$, $J_0(.)$ is the Bessel function of the first kind of zero order. Eq. (22) can be written in the more suitable form as:

$$\overline{w}_H(r_n,s) = \frac{b_0}{c_n}\left[(1-Ga_{1n})\frac{s^{-1}}{s^{\alpha}+a_{1n}} - (1-Ga_{2n})\frac{s^{-1}}{s^{\alpha}+a_{2n}}\right]\frac{J_1(r_n)}{r_n} + \frac{b_1}{c_n}\frac{s}{s^2+\omega^2}\left[(1-Ga_{1n})\frac{1}{s^{\alpha}+a_{1n}} - (1-Ga_{2n})\frac{1}{s^{\alpha}+a_{2n}}\right]\frac{J_1(r_n)}{r_n}. \quad (23)$$

Where;

$$a_{1n} = \frac{b_n - c_n}{2G},\ a_{2n} = \frac{b_n + c_n}{2G},\ b_n = 1 + G(R+H) + \beta_1 r_n^{\ 2}G,$$

$$c_n = \sqrt{b_n^{\ 2} - 4G(H + \beta_1 r_n^{\ 2})}.$$

Using the particular functions to get the inverse Laplace transform of Eq. (23):

$$L^{-1}[\frac{1}{s^{\alpha}+m}] = F_{\alpha}(-m,t) = \sum_{n=0}^{\infty}\frac{(-m)^n t^{(n+1)\alpha-1}}{\Gamma(\alpha(n+1))}, \quad (24)$$

$$L^{-1}[\frac{s^{\eta}}{s^{\alpha}+m}] = R_{\alpha}(-m,t) = \sum_{n=0}^{\infty}\frac{(-m)^n t^{(n+1)\alpha-1-\eta}}{\Gamma(\alpha(n+1)-\eta)}. \quad (25)$$

Where $F_\alpha(.,.)$ and $R_\alpha(.,.)$ are the Robotnov-Hartley's and the Lorenzo-Hartley's functions respectively [47], we get:

$$w(r,t)=2\sum_{n=1}^{\infty}\frac{J_0(rr_n)}{r_nJ_1(r_n)}[F_{1n}(t)+F_{2n}(t)], \tag{26}$$

$$F_{1n}(t)=\frac{b_0}{c_n}[(1-Ga_{1n})R_{\alpha,-1}(-a_{1n},t)-(1-Ga_{2n})R_{\alpha,-1}(-a_{2n},t)], \tag{27}$$

$$F_{2n}(t)=\frac{b_1}{c_n}\cos(\omega t)[(1-Ga_{1n})F_\alpha(-a_{1n},t)-(1-Ga_{2n})F_\alpha(-a_{2n},t)]. \tag{28}$$

3.2. Calculation of Energy

Applying the Laplace transform to Eq. (15), and Eq. (16), we obtain:

$$\begin{aligned}s^\alpha\overline{T}(r,s)&=\frac{1}{P_e}\left(\frac{\partial^2\overline{T}(r,s)}{\partial r^2}+\frac{1}{r}\frac{\partial\overline{T}(r,s)}{\partial r}\right)-4\frac{R_a}{P_e}\overline{T}(r,s)\\&+\frac{B_r}{P_e}\left(\frac{\partial\overline{w}(r,s)}{\partial r}\right)^2+\frac{R_s}{P_e}\left\{\overline{T}_s(r,s)-\overline{T}(r,s)\right\},\end{aligned} \tag{29}$$

$$\overline{T}_s(r,s)=\frac{\gamma}{s^\alpha+\gamma}\overline{T}(r,s), \tag{30}$$

Incorporating Eq. (30) into Eq. (29), we get:

$$\begin{aligned}s^\alpha\overline{T}(r,s)&=\frac{1}{P_e}\left(\frac{\partial^2\overline{T}(r,s)}{\partial r^2}+\frac{1}{r}\frac{\partial\overline{T}(r,s)}{\partial r}\right)-4\frac{R_a}{P_e}\overline{T}(r,s)\\&+\frac{B_r}{P_e}\left(\frac{\partial\overline{w}(r,s)}{\partial r}\right)^2+\frac{R_s}{P_e}\left(\frac{\gamma}{s^\alpha+\gamma}\overline{T}(r,s)-\overline{T}(r,s)\right).\end{aligned} \tag{31}$$

Applying the Hankel transform of order zero in Eq. (31), and then inserting Eq. (23) for $\overline{w}_H(r_n,s)$, we obtain:

$$\begin{aligned}\overline{T}_H(r_n,s)&=\frac{J_1(r_n)}{r_n}+A_{n4}\left(\frac{b_0}{s}+\frac{b_1s}{s^2+\omega^2}\right)\left[\frac{\gamma-\alpha_{n1}}{s^\alpha+\alpha_{n1}}-\frac{\gamma-\alpha_{n2}}{s^\alpha+\alpha_{n2}}\right]\\&\frac{\partial}{\partial r_n}\left[\left(\frac{1-Ga_{1n}}{s^\alpha+a_{1n}}-\frac{1-Ga_{2n}}{s^\alpha+a_{2n}}\right)\left(\frac{J_1(r_n)}{r_nc_n}\right)\right]\\&+\left(\frac{J_1(r_n)}{r_n}\right)\left[\frac{An1}{s}+\frac{(\gamma-\alpha_{n1})A_{n2}s^{-1}}{(s^\alpha+\alpha_{n1})}+\frac{(\gamma-\alpha_{n2})A_{n3}s^{-1}}{(s^\alpha+\alpha_{n2})}\right].\end{aligned} \tag{32}$$

Where;

$$\begin{aligned}&b_{n1}=\frac{P_e\gamma+r_n^2+4R_a+R_s}{P_e},\ \alpha_1=\frac{r_n^2\gamma+4R_a\gamma}{P_e},\ c_{n1}=\sqrt{(b_{n1})^2-4\alpha_1},\\&\alpha_{n1}=\frac{b_{n1}-c_{n1}}{2},\ \alpha_{n2}=\frac{b_{n1}+c_{n1}}{2},\ A_{n1}=\frac{r_n^2\gamma-\alpha_{n1}\alpha_{n2}P_e}{P_e\alpha_{n1}\alpha_{n2}},\\&A_{n2}=\frac{r_n^2}{P_e(\alpha_{n2}-\alpha_{n1})},\ A_{n3}=\frac{r_n^2}{P_e(\alpha_{n1}-\alpha_{n2})},\ A_{n4}=\frac{2B_r}{c_nP_e}.\end{aligned} \tag{33}$$

The Bessel expansion is given by:

$$J_{n+1}(x)=\frac{nJ_n(x)}{x}-J_n'(x),\ \text{and}\ J_{n+1}(x)-J_{n-1}(x)=-2J_n'(x), \tag{34}$$

$$-\left(\frac{J_1(r_n)}{r_nc_n}\right)=-\frac{J_2(r_n)}{r_nc_n}-\frac{c_n'}{c_n^2}\left\{J_2(r_n)+J_1'(r_n)\right\}, \tag{35}$$

$$\begin{aligned}\frac{\partial}{\partial r_n}\left[\frac{1-Ga_{1n}}{s^\alpha+a_{1n}}-\frac{1-Ga_{2n}}{s^\alpha+a_{2n}}\right]&=\frac{-a_{1n}'G(s^\alpha+a_{1n})-a_{1n}'(1-a_{1n}G)}{(s^\alpha+a_{1n})^2}\\&+\frac{a_{2n}'G(s^\alpha+a_{2n})+a_{2n}'(1-a_{2n}G)}{(s^\alpha+a_{2n})^2}.\end{aligned} \tag{36}$$

Equation (35), and Eq. (36), employed in Eq. (32) and expended, we get:

$$\begin{aligned}\overline{T}_{H_1}(r_n,s)&=\frac{J_1(r_n)}{r_n}\\&+A_{n4}b_0\frac{c_n'}{c_n^2}\frac{J_1(r_n)}{r_n}\begin{bmatrix}\frac{s^{-1}(\gamma-\alpha_{n1})(1-Ga_{1n})}{(s^\alpha+k_{n2})(s^\alpha+k_{n1})}-\frac{s^{-1}(\gamma-\alpha_{n1})(1-Ga_{2n})}{(s^\alpha+k_{n4})(s^\alpha+k_{n3})}\\-\frac{s^{-1}(\gamma-\alpha_{n2})(1-Ga_{1n})}{(s^\alpha+k_{n6})(s^\alpha+k_{n5})}+\frac{s^{-1}(\gamma-\alpha_{n2})(1-Ga_{2n})}{(s^\alpha+k_{n8})(s^\alpha+k_{n7})}\end{bmatrix}\\&+A_{n4}b_1\frac{c_n'}{c_n^2}\frac{s}{s^2+\omega^2}\frac{J_1(r_n)}{r_n}\begin{bmatrix}\frac{(\gamma-\alpha_{n1})(1-Ga_{1n})}{(s^\alpha+k_{n2})(s^\alpha+k_{n1})}-\frac{(\gamma-\alpha_{n1})(1-Ga_{2n})}{(s^\alpha+k_{n4})(s^\alpha+k_{n3})}\\-\frac{(\gamma-\alpha_{n2})(1-Ga_{1n})}{(s^\alpha+k_{n6})(s^\alpha+k_{n5})}+\frac{(\gamma-\alpha_{n2})(1-Ga_{2n})}{(s^\alpha+k_{n8})(s^\alpha+k_{n7})}\end{bmatrix}\\&+A_{n4}\frac{b_0}{c_n}\frac{J_2(r_n)}{r_n}\begin{bmatrix}\frac{s^{-1}(\gamma-\alpha_{n1})(1-Ga_{2n})}{(s^\alpha+k_{n4})(s^\alpha+k_{n3})}-\frac{s^{-1}(\gamma-\alpha_{n1})(1-Ga_{1n})}{(s^\alpha+k_{n2})(s^\alpha+k_{n1})}\\+\frac{s^{-1}(\gamma-\alpha_{n2})(1-Ga_{1n})}{(s^\alpha+k_{n6})(s^\alpha+k_{n5})}-\frac{s^{-1}(\gamma-\alpha_{n2})(1-Ga_{2n})}{(s^\alpha+k_{n8})(s^\alpha+k_{n7})}\end{bmatrix}\\&+\frac{A_{n4}b_1}{c_n}\frac{s}{s^2+\omega^2}\frac{J_2(r_n)}{r_n}\begin{bmatrix}\frac{(\gamma-\alpha_{n1})(1-Ga_{2n})}{(s^\alpha+k_{n4})(s^\alpha+k_{n3})}-\frac{(\gamma-\alpha_{n1})(1-Ga_{1n})}{(s^\alpha+k_{n2})(s^\alpha+k_{n1})}\\+\frac{(\gamma-\alpha_{n2})(1-Ga_{1n})}{(s^\alpha+k_{n6})(s^\alpha+k_{n5})}-\frac{(\gamma-\alpha_{n2})(1-Ga_{2n})}{(s^\alpha+k_{n8})(s^\alpha+k_{n7})}\end{bmatrix},\end{aligned} \tag{37}$$

$$\begin{aligned}\overline{T}_{H_2}(r_n,s)&=\frac{A_{n4}b_0}{c_n}\frac{J_1(r_n)}{r_n}\begin{bmatrix}-\frac{s^{-1}a_{1n}'G(\gamma-\alpha_{n1})}{(s^\alpha+k_{n2})(s^\alpha+k_{n1})}-\frac{s^{-1}a_{1n}'(1-a_{1n}G)(\gamma-\alpha_{n1})}{(s^\alpha+k_{n2})(s^\alpha+k_{n1})(s^\alpha+a_{1n})}\\+\frac{s^{-1}a_{1n}'G(\gamma-\alpha_{n2})}{(s^\alpha+k_{n6})(s^\alpha+k_{n5})}+\frac{s^{-1}a_{1n}'(1-a_{1n}G)(\gamma-\alpha_{n2})}{(s^\alpha+k_{n6})(s^\alpha+k_{n5})(s^\alpha+a_{1n})}\\+\frac{s^{-1}a_{2n}'G(\gamma-\alpha_{n1})}{(s^\alpha+k_{n4})(s^\alpha+k_{n3})}+\frac{s^{-1}a_{2n}'(1-a_{2n}G)(\gamma-\alpha_{n1})}{(s^\alpha+k_{n4})(s^\alpha+k_{n3})(s^\alpha+a_{2n})}\\-\frac{s^{-1}a_{2n}'G(\gamma-\alpha_{n2})}{(s^\alpha+k_{n8})(s^\alpha+k_{n7})}-\frac{s^{-1}a_{2n}'(1-a_{2n}G)(\gamma-\alpha_{n2})}{(s^\alpha+k_{n8})(s^\alpha+k_{n7})(s^\alpha+a_{2n})}\end{bmatrix},\\&+\frac{A_{n4}b_1}{c_n}\frac{s}{s^2+\omega^2}\frac{J_1(r_n)}{r_n}\begin{bmatrix}-\frac{a_{1n}'G(\gamma-\alpha_{n1})}{(s^\alpha+k_{n2})(s^\alpha+k_{n1})}-\frac{a_{1n}'(1-a_{1n}G)(\gamma-\alpha_{n1})}{(s^\alpha+k_{n2})(s^\alpha+k_{n1})(s^\alpha+a_{1n})}\\+\frac{a_{1n}'G(\gamma-\alpha_{n2})}{(s^\alpha+k_{n6})(s^\alpha+k_{n5})}+\frac{a_{1n}'(1-a_{1n}G)(\gamma-\alpha_{n2})}{(s^\alpha+k_{n6})(s^\alpha+k_{n5})(s^\alpha+a_{1n})}\\+\frac{a_{2n}'G(\gamma-\alpha_{n1})}{(s^\alpha+k_{n4})(s^\alpha+k_{n3})}+\frac{a_{2n}'(1-a_{2n}G)(\gamma-\alpha_{n1})}{(s^\alpha+k_{n4})(s^\alpha+k_{n3})(s^\alpha+a_{2n})}\\-\frac{a_{2n}'G(\gamma-\alpha_{n2})}{(s^\alpha+k_{n8})(s^\alpha+k_{n7})}-\frac{a_{2n}'(1-a_{2n}G)(\gamma-\alpha_{n2})}{(s^\alpha+k_{n8})(s^\alpha+k_{n7})(s^\alpha+a_{2n})}\end{bmatrix}\end{aligned} \tag{38}$$

$$\overline{T}_{H_3}(r_n,s)=\frac{J_1(r_n)}{r_n}\left(\frac{A_{n1}}{s}+\frac{A_{n2}(\gamma-\alpha_{n1})s^{-1}}{(s^{\alpha}+\alpha_{n1})}+\frac{A_{n3}(\gamma-\alpha_{n2})s^{-1}}{(s^{\alpha}+\alpha_{n2})}\right). \quad (39)$$

Where;

$$b_{n2}=a_{1n}+\alpha_{n1},\ c_{n2}=\sqrt{(b_{n2})^2-4\alpha_{n1}a_{1n}},\ k_{n1}=\frac{b_{n2}-c_{n2}}{2},$$

$$k_{n2}=\frac{b_{n2}+c_{n2}}{2},\ b_{n3}=a_{2n}+\alpha_{n1},\ c_{n3}=\sqrt{(b_{n3})^2-4\alpha_{n1}a_{2n}},$$

$$k_{n3}=\frac{b_{n3}-c_{n3}}{2},\ k_{n4}=\frac{b_{n3}+c_{n3}}{2},\ b_{n4}=a_{1n}+\alpha_{n2},$$

$$c_{n4}=\sqrt{(b_{n4})^2-4\alpha_{n2}a_{1n}},\ k_{n5}=\frac{b_{n4}-c_{n4}}{2},$$

$$k_{n6}=\frac{b_{n4}+c_{n4}}{2},\ b_{n5}=a_{2n}+\alpha_{n2},\ c_{n5}=\sqrt{(b_{n5})^2-4\alpha_{n2}a_{2n}},$$

$$k_{n7}=\frac{b_{n5}-c_{n5}}{2},\ k_{n8}=\frac{b_{n5}+c_{n5}}{2}. \quad (40)$$

By applying Eq. (24) and Eq. (25) to Eqs. (37), (38), and Eq. (39), we obtain:

$$T_1(r,t)=1+2\sum_{n=1}^{\infty}\left[\begin{array}{l}\dfrac{J_0(rr_n)}{r_nJ_1(r_n)}\{F_{3n}(t)+F_{4n}(t)\}\\+\dfrac{J_0(rr_n)J_2(r_n)}{r_nJ_1^2(r_n)}\{F_{5n}(t)+F_{6n}(t)\}\end{array}\right], \quad (41)$$

$$T_2(r,t)=2\sum_{n=1}^{\infty}\frac{J_0(rr_n)}{r_nJ_1(r_n)}\left[\begin{array}{l}F_{7n}(t)+F_{8n}(t)+F_{9n}(t)+F_{10n}(t)+\\F_{11n}(t)+F_{12n}(t)+F_{13n}(t)+F_{14n}(t)\end{array}\right], \quad (42)$$

$$T_3(r,t)=2\sum_{n=1}^{\infty}\frac{J_0(rr_n)}{r_nJ_1(r_n)}\left[A_{n1}+F_{15n}(t)+F_{16n}(t)\right]. \quad (43)$$

Where;

$$F_{3n}(t)=\frac{A_{n4}b_0c_n'}{c_n^2}\frac{J_1(r_n)}{r_n}\left[\begin{array}{l}(\gamma-\alpha_{n1})(1-Ga_{1n})R_{\alpha,-1}(-k_{n2},t)F_{\alpha}(-k_{n1},t)\\-(\gamma-\alpha_{n2})(1-Ga_{1n})R_{\alpha,-1}(-k_{n4},t)F_{\alpha}(-k_{n3},t)\\-(\gamma-\alpha_{n2})(1-Ga_{1n})R_{\alpha,-1}(-k_{n6},t)F_{\alpha}(-k_{n5},t)\\+(\gamma-\alpha_{n2})(1-Ga_{2n})R_{\alpha,-1}(-k_{n8},t)F_{\alpha}(-k_{n7},t)\end{array}\right],$$

$$F_{4n}(t)=\frac{A_{n4}b_1c_n'}{c_n^2}\mathrm{Cos}\,\omega t\left[\begin{array}{l}(\gamma-\alpha_{n1})(1-Ga_{1n})F_{\alpha}(-k_{n2},t)F_{\alpha}(-k_{n1},t)\\-(\gamma-\alpha_{n2})(1-Ga_{1n})F_{\alpha}(-k_{n4},t)F_{\alpha}(-k_{n3},t)\\-(\gamma-\alpha_{n2})(1-Ga_{1n})F_{\alpha}(-k_{n6},t)F_{\alpha}(-k_{n5},t)\\+(\gamma-\alpha_{n2})(1-Ga_{2n})F_{\alpha}(-k_{n8},t)F_{\alpha}(-k_{n7},t)\end{array}\right],$$

$$F_{5n}(t)=\frac{A_{n4}b_0}{c_n}\left[\begin{array}{l}(\gamma-\alpha_{n2})(1-Ga_{1n})R_{\alpha,-1}(-k_{n4},t)F_{\alpha}(-k_{n3},t)\\-(\gamma-\alpha_{n1})(1-Ga_{1n})R_{\alpha,-1}(-k_{n2},t)F_{\alpha}(-k_{n1},t)\\+(\gamma-\alpha_{n2})(1-Ga_{1n})R_{\alpha,-1}(-k_{n6},t)F_{\alpha}(-k_{n5},t)\\-(\gamma-\alpha_{n2})(1-Ga_{2n})R_{\alpha,-1}(-k_{n8},t)F_{\alpha}(-k_{n7},t)\end{array}\right],$$

$$F_{6n}(t)=\frac{A_{n4}b_1}{c_n}\mathrm{Cos}\,\omega t\left[\begin{array}{l}(\gamma-\alpha_{n2})(1-Ga_{1n})F_{\alpha}(-k_{n4},t)F_{\alpha}(-k_{n3},t)\\-(\gamma-\alpha_{n1})(1-Ga_{1n})F_{\alpha}(-k_{n2},t)F_{\alpha}(-k_{n1},t)\\+(\gamma-\alpha_{n2})(1-Ga_{1n})F_{\alpha}(-k_{n6},t)F_{\alpha}(-k_{n5},t)\\-(\gamma-\alpha_{n2})(1-Ga_{2n})F_{\alpha}(-k_{n8},t)F_{\alpha}(-k_{n7},t)\end{array}\right],$$

$$F_{7n}(t)=\frac{A_{n4}b_0}{c_n}G(\gamma-\alpha_{n1})\left[\begin{array}{l}a_{2n}'R_{a,-1}(-k_{n4},t)F_a(-k_{n3},t)\\-a_{1n}'R_{a,-1}(-k_{n2},t)F_a(-k_{n1},t)\end{array}\right],$$

$$F_{8n}(t)=\frac{A_{n4}b_0}{c_n}G(\gamma-\alpha_{n2})\left[\begin{array}{l}a_{1n}'R_{\alpha,-1}(-k_{n6},t)F_{\alpha}(-k_{n5},t)\\-a_{2n}'R_{\alpha,-1}(-k_{n8},t)F_{\alpha}(-k_{n7},t)\end{array}\right],$$

$$F_{9n}(t)=\frac{A_{n4}b_0}{c_n}(\gamma-\alpha_{n1})\left[\begin{array}{l}a_{2n}'R_{\alpha,-1}(-k_{n4},t)F_{\alpha}(-k_{n3},t)F_{\alpha}(-a_{2n},t)(1-a_{2n}G)\\-a_{1n}'R_{\alpha,-1}(-k_{n2},t)F_{\alpha}(-k_{n1},t)F_{\alpha}(-a_{1n},t)(1-a_{1n}G)\end{array}\right],$$

$$F_{10n}(t)=\frac{A_{n4}b_0}{c_n}(\gamma-\alpha_{n2})\left[\begin{array}{l}a_{1n}'R_{\alpha,-1}(-k_{n6},t)F_{\alpha}(-k_{n5},t)F_{\alpha}(-a_{1n},t)(1-a_{1n}G)\\-a_{2n}'R_{\alpha,-1}(-k_{n8},t)F_{\alpha}(-k_{n7},t)F_{\alpha}(-a_{2n},t)(1-a_{2n}G)\end{array}\right],$$

$$F_{11n}(t)=\frac{A_{n4}b_1}{c_n}G\,\mathrm{Cos}\,\omega t(\gamma-\alpha_{n1})\left[\begin{array}{l}a_{2n}'F_{\alpha}(-k_{n4},t)F_{\alpha}(-k_{n3},t)\\-a_{1n}'F_{\alpha}(-k_{n2},t)F_{\alpha}(-k_{n1},t)\end{array}\right],$$

$$F_{12n}(t)=\frac{A_{n4}b_1}{c_n}G\,\mathrm{Cos}\,\omega t(\gamma-\alpha_{n2})\left[\begin{array}{l}a_{1n}'F_{\alpha}(-k_{n6},t)F_{\alpha}(-k_{n5},t)\\-a_{2n}'F_{\alpha}(-k_{n8},t)F_{\alpha}(-k_{n7},t)\end{array}\right],$$

$$F_{13n}(t)=\frac{A_{n4}b_1}{c_n}\mathrm{Cos}\,\omega t(\gamma-\alpha_{n1})$$
$$\left[\begin{array}{l}a_{2n}'(1-a_{2n}G)R_{\alpha,-1}(-k_{n4},t)F_{\alpha}(-k_{n3},t)F_{\alpha}(-a_{2n},t)\\-a_{1n}'(1-a_{1n}G)R_{\alpha,-1}(-k_{n2},t)F_{\alpha}(-k_{n1},t)F_{\alpha}(-a_{1n},t)\end{array}\right]$$

$$F_{14n}(t)=\frac{A_{n4}b_1}{c_n}\mathrm{Cos}\,\omega t(\gamma-\alpha_{n2})$$
$$\left[\begin{array}{l}a_{1n}'(1-a_{1n}G)R_{\alpha,-1}(-k_{n6},t)F_{\alpha}(-k_{n5},t)F_{\alpha}(-a_{1n},t)\\-a_{2n}'(1-a_{2n}G)R_{\alpha,-1}(-k_{n8},t)F_{\alpha}(-k_{n7},t)F_{\alpha}(-a_{2n},t)\end{array}\right],$$

$$F_{15n}(t)=A_{n2}(\gamma-\alpha_{n1})R_{a,-1}(-\alpha_{n1},t),$$

$$F_{16n}(t)=A_{n3}(\gamma-\alpha_{n2})R_{\alpha,-1}(-\alpha_{n2},t).$$

4. Graphical Results

To understand the influence of various embedded parameters on the blood velocity $w(r, t)$, particle velocity $w_1(r, t)$, the Temperature of blood $T(r, t)$, and the particle's temperature $T_s(r, t)$, various graphs are plotted using Mathcad software. Fig. 2 is plotted to represent the behavior of fractional parameter α on both the velocities of blood and particles for a small time ($t = 0.05$) and large time ($t = 2$). It is observed that for a shorter and larger time, the opposite behavior is noticed. The fractional parameter α provides multiple integral curves when its value is ($0 < \alpha < 1$), than the classical solution ($\alpha = 1$).

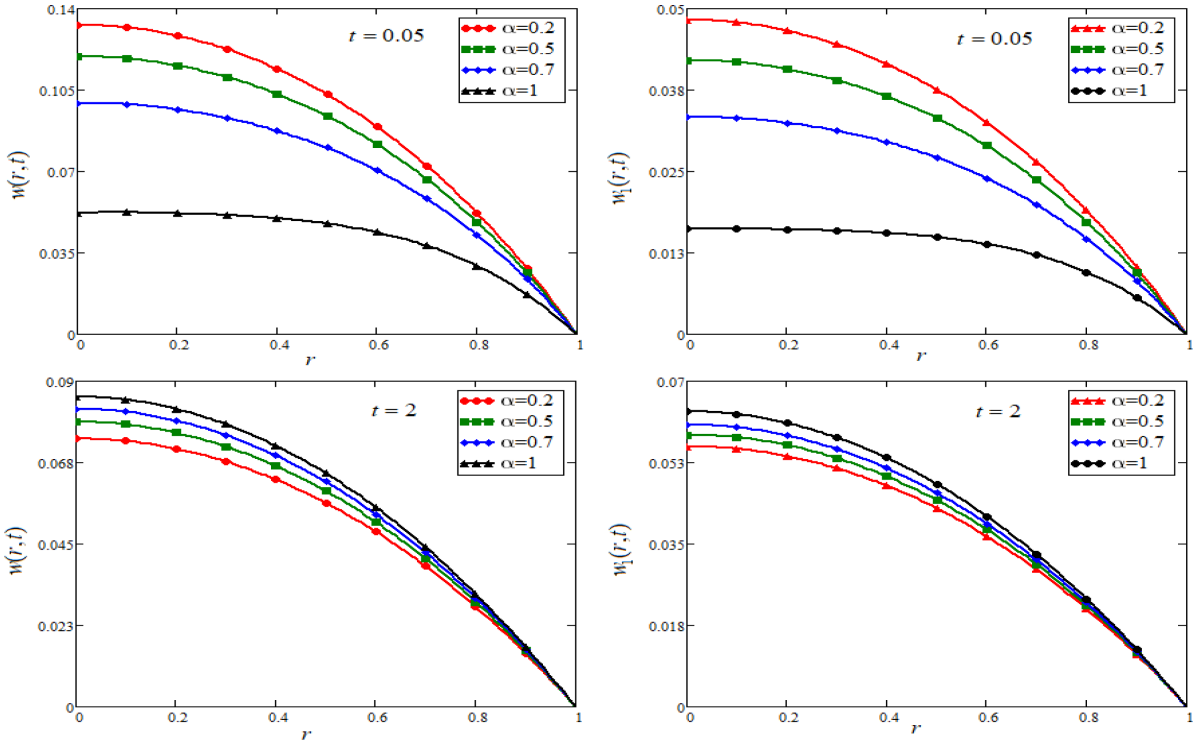

Fig. 2. (Color online) Profiles for the velocity of blood and particles for $t = 0.05$ & $t = 2$, at different values of α when, $b_0 = 0.5$, $b_1 = 0.6$, Re = 3, $G = 0.8$, $R = 0.5$, $\beta = 0.4$ and $H = 1$.

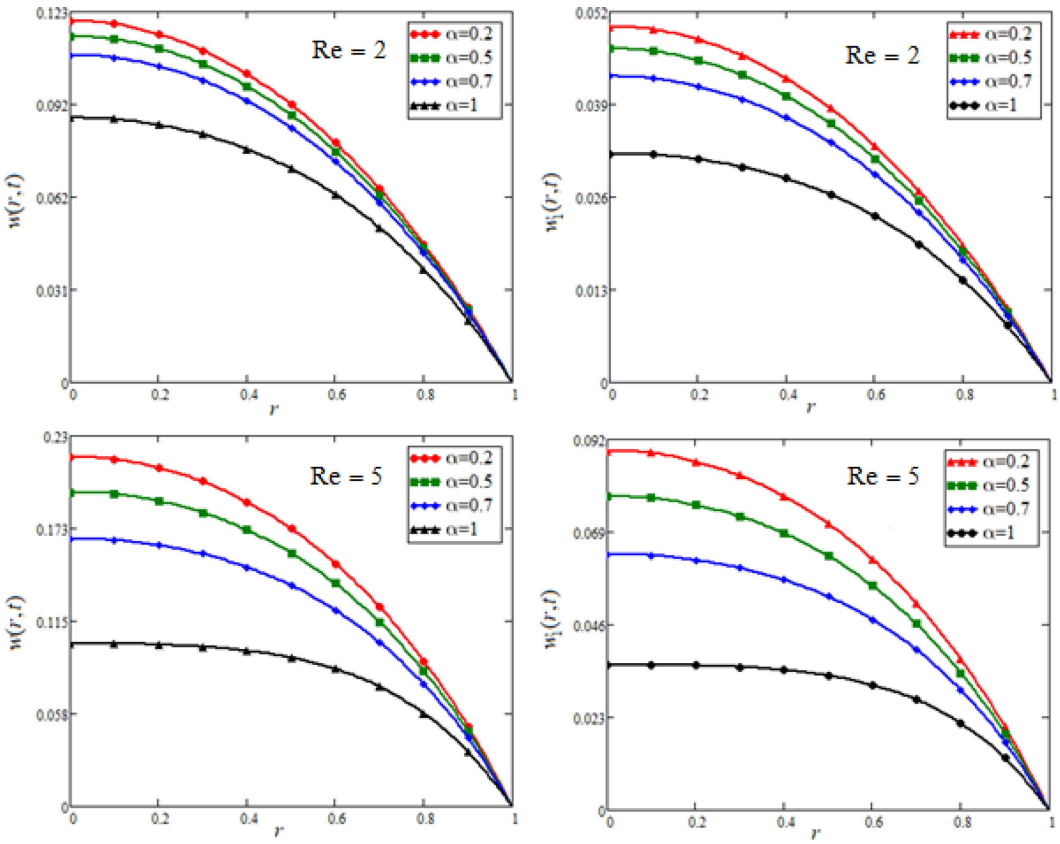

Fig. 3. (Color online) Profiles for the velocity of blood and particles at time $t = 0.1$ and different values of Re when, $b_0 = 0.5$, $b_1 = 0.6$, $G = 0.8$, $R = 0.5$, $H = 1$ and $\beta = 0.4$.

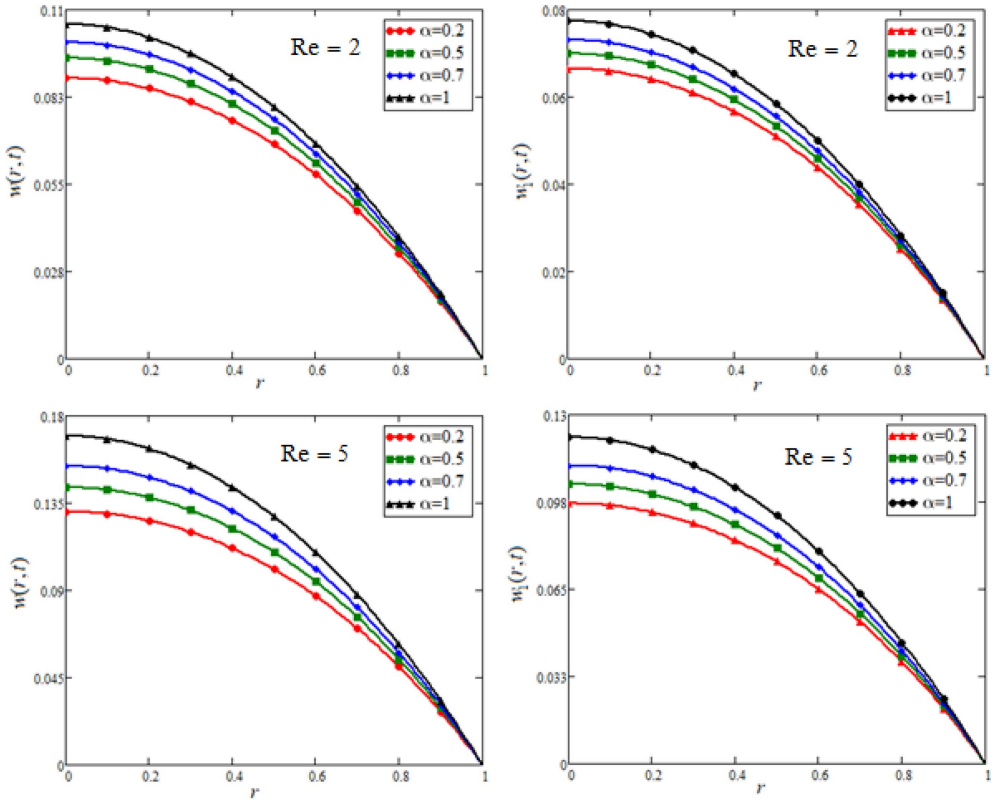

Fig. 4. (Color online) Profiles for velocity of blood and particles at time $t = 2$ and different values of Re when, $b_0 = 0.5$, $b_1 = 0.6$, $G = 0.8$, $R = 0.5$, $H = 1$ and $\beta = 0.4$.

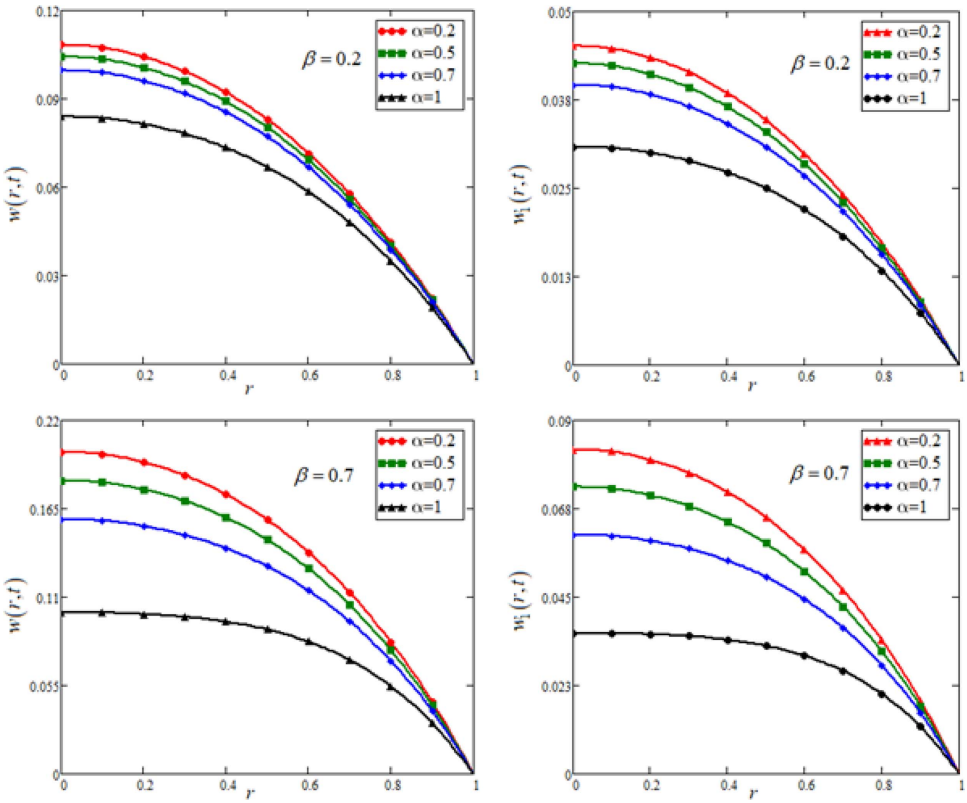

Fig. 5. (Color online) Profiles for velocity of blood and particles at time $t = 0.1$ and different values of β when, Re = 3, $b_0 = 0.5$, $b_1 = 0.6$, $G = 0.8$, and $H = 1$.

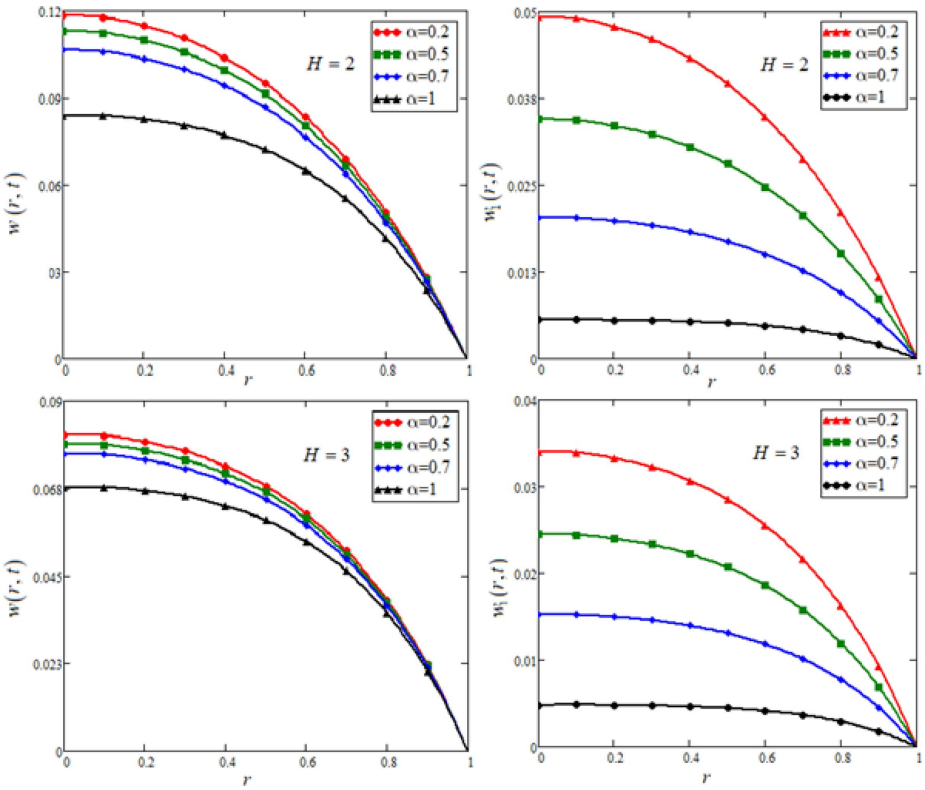

Fig. 6. (Color online) Profiles for velocity of blood and particles at time $t = 0.1$ and different values of H when $b_0 = 0.5$, $b_1 = 0.6$, $G = 0.8$, $\beta = 0.4$, and $\mathrm{Re} = 3$.

These multiple solutions may be used to best fit the theoretical solutions with the real data. This shows the fractional-order model is more general than the classical order model. Figs. 3 & 4 show the influence of Re on the velocities of blood and particles. The blood and particles velocities increase with enhancing values of Re. Physically, it is true because Re is the ratio of arterial radius and viscosity of the blood. Therefore, the blood becomes thinner by increasing Re, and hence the velocity of the blood and particles increases, which is significant in decreasing the blood pressure and in the supply of heat to the tissues of the body and carrying drugs to the affected tissues. In Fig. 5 Both the blood velocity and particle velocity increase by increasing the values of β, because when the values of β increase, the yield stress decreases and therefore the thickness of the blood decreases. Figs. 6 and 7 show the effect of the magnetic parameter or Hartmann number H on both the particle and blood velocities. By increasing the values of H both velocities decrease. It is true because by applying a magnetic field on a moving electrically conducting fluid, the Lorentz forces are produced due to the interaction of the magnetic field and induced currents that retard the blood flow. By regulating the intensity of the applied external magnetic field is useful to control the blood flow during magnetic therapy (for treating pain, such as the back, foot, or joint pain) and surgeries.

Figure 8 is plotted to represent the behavior of fractional order parameter α on both the temperature of blood and particles for small-time ($t = 0.1$) and large time ($t = 2$). The behavior of α on temperature of blood and particle is reported same as for the blood and particle velocities. Therefore, this may be a tool to control the blood and particle temperatures during treatment by using the suitable values of α for regulating blood and particles temperature. Figs. 9 and 10, represent the increase in temperature of both the blood and particle by increasing the values of Peclet number. As the Peclet number is the ratio of advection to diffusion, so by increasing the Peclet number the advection becomes dominant due to which temperature of the blood and particles increase, because advection is the transport of a substance by bulk motion and the properties of that substance are carried with it. Figs. 11, and 12, show the decrease in temperature of blood and particle by increasing the values of R_a. The blood and particle temperature is maximum at the center of the vessel and minimum at the walls of the vessel, which is significant to avoid effecting the tissues during

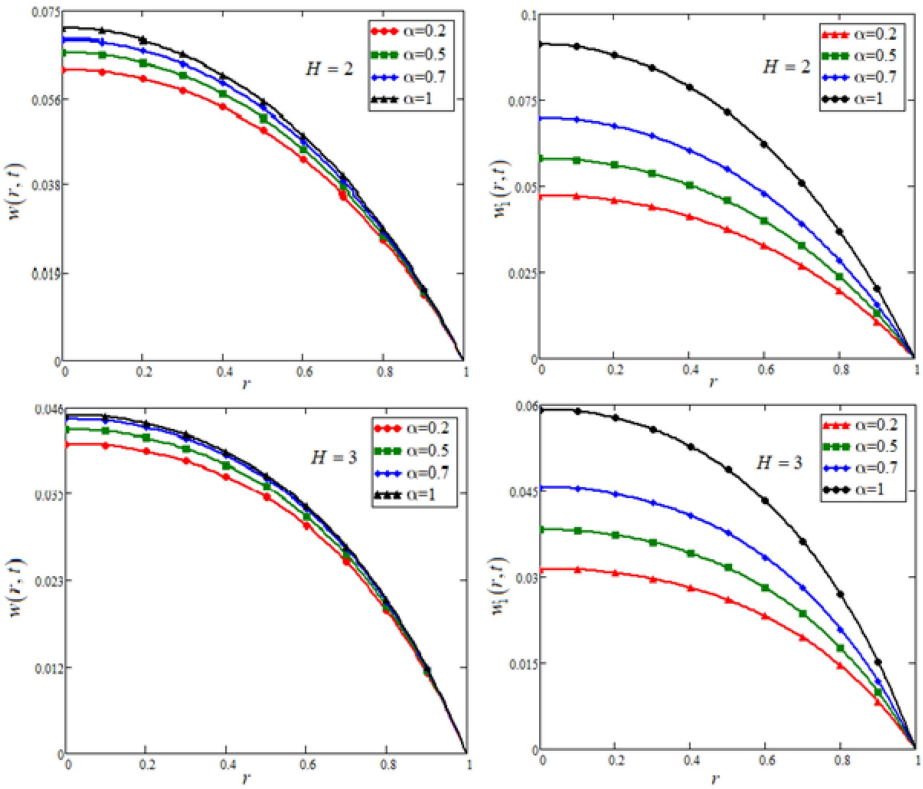

Fig. 7. (Color online) Profiles for velocity of blood and particles at time $t = 2$ and different values of H, when $b_0 = 0.5$, $b_1 = 0.6$, Re = 3, $G = 0.8$, $R = 0.5$, and $\beta = 0.4$.

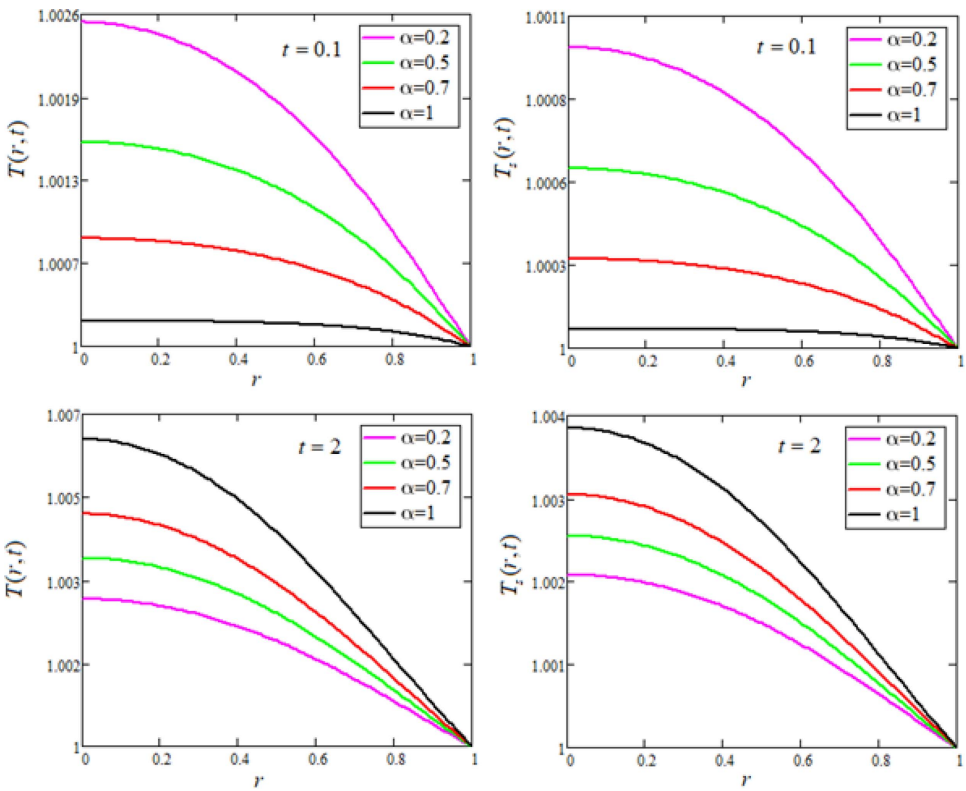

Fig. 8. (Color online) Profiles for temperature of blood and particles at small and large values of time t when $P_e = 5$, $R_a = 0.1$ $B_r = 0.1$ and $R_s = 5$.

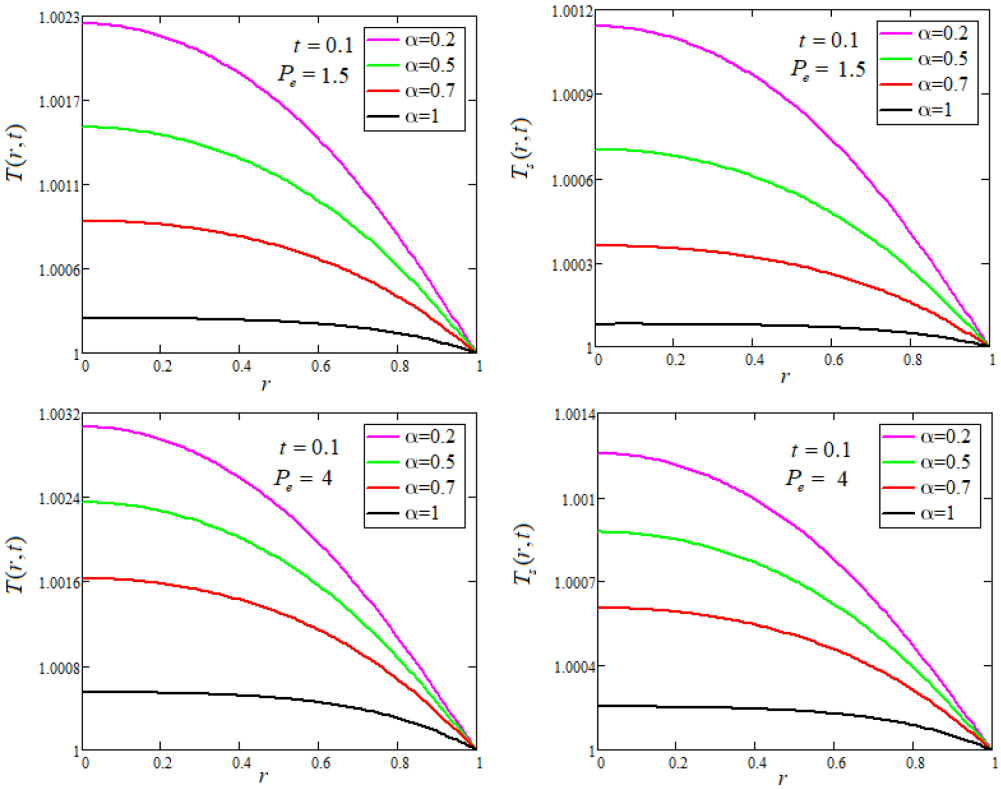

Fig. 9. (Color online) Profiles for Temperature of blood and particles at different values P_e at $t = 0.1$ when $R_a = 0.1$, $B_r = 0.1$ and $R_s = 5$.

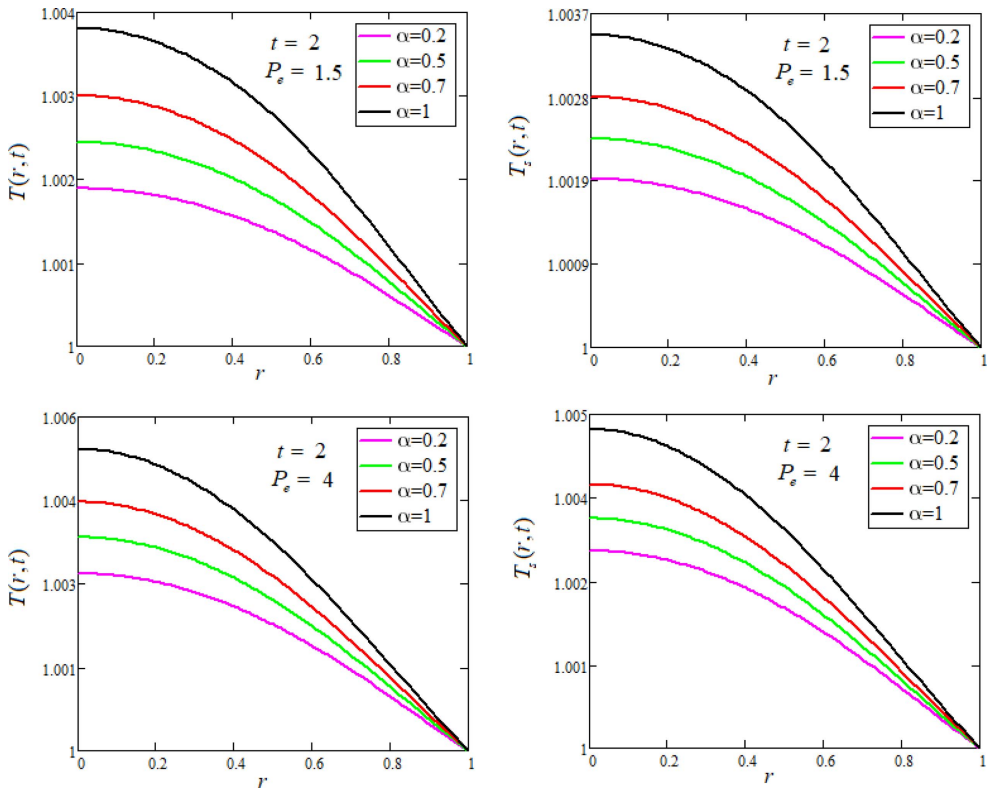

Fig. 10. (Color online) Profiles for temperature of blood and particles at different values P_e at $t = 2$ when $R_a = 0.1$, $B_r = 0.1$ and $R_s = 5$.

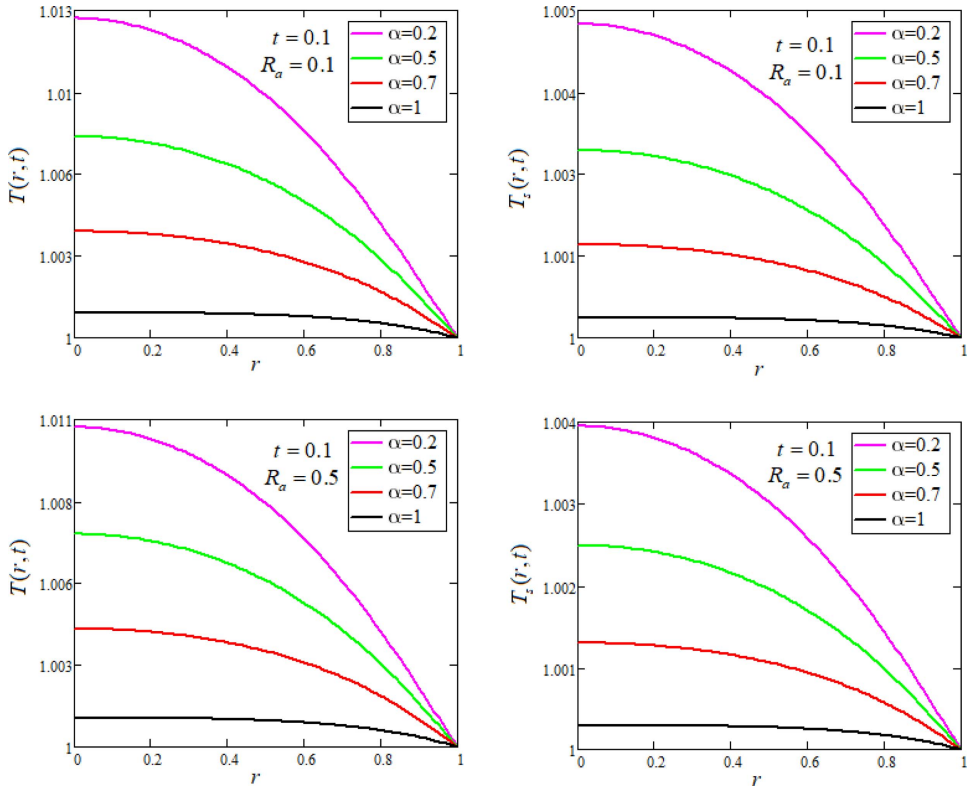

Fig. 11. (Color online) Profiles for temperature of blood and particles at different values R_a at $t = 0.1$ when $Pe = 0.5$, $B_r = 0.1$ and $R_s = 5$.

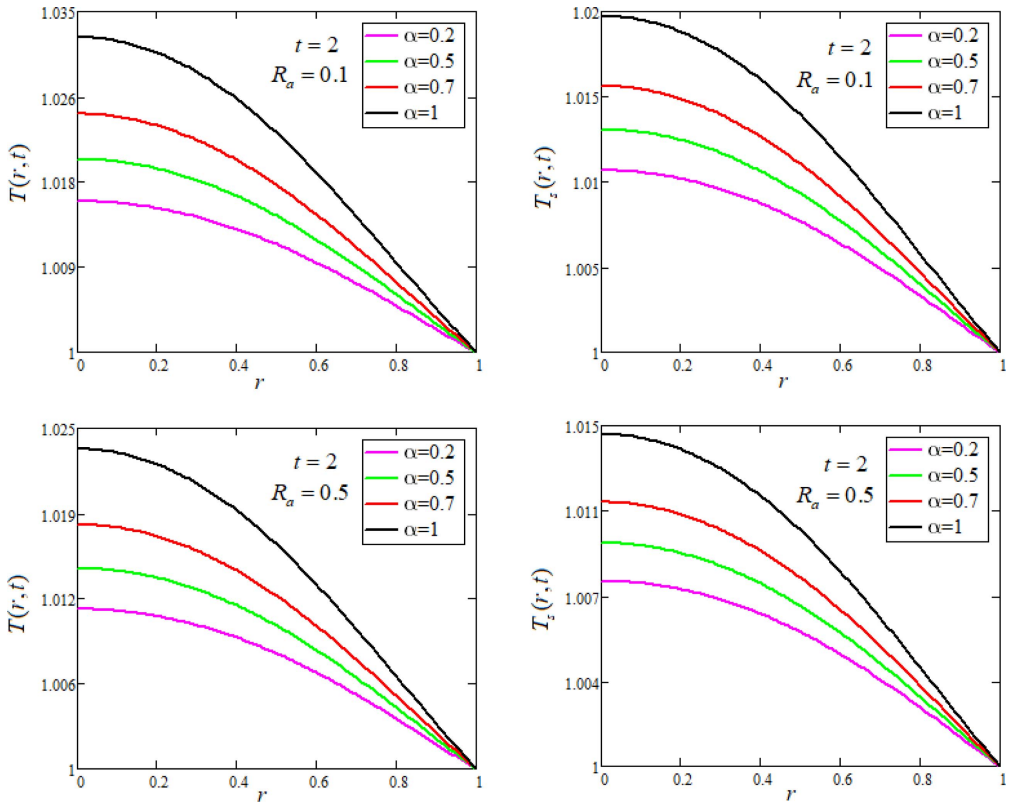

Fig. 12. (Color online) Profiles for temperature of blood and particles at different values R_a at $t = 2$ when $Pe = 10$, $B_r = 0.1$ and $R_s = 5$.

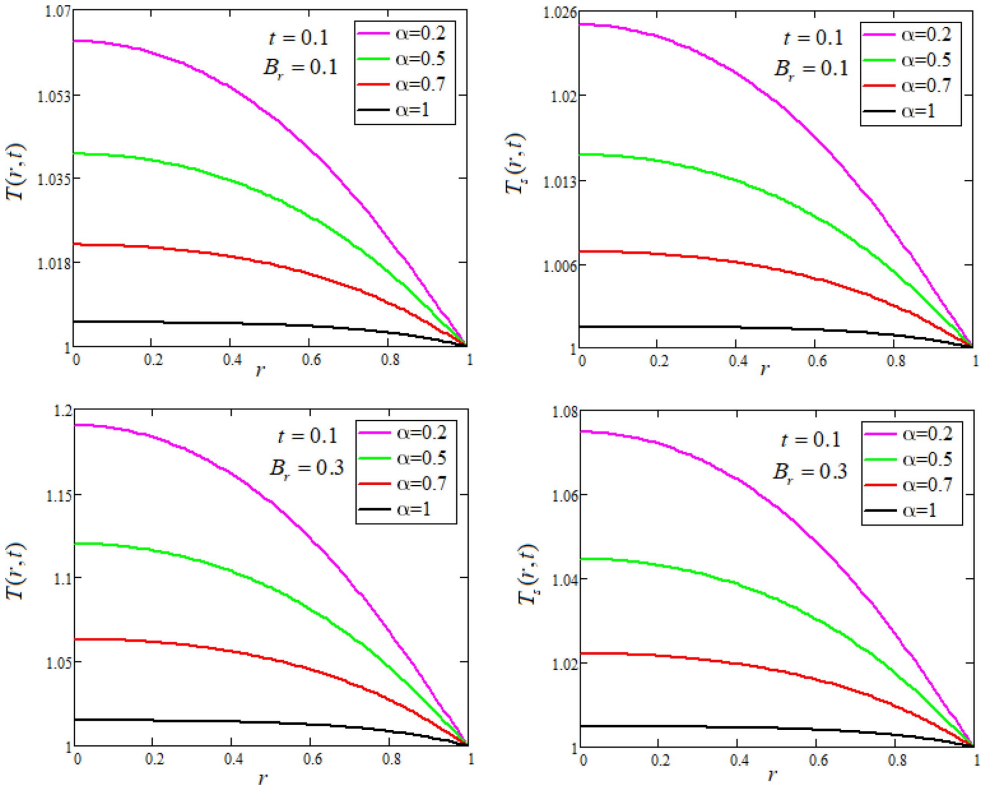

Fig. 13. (Color online) Profiles for temperature of blood and particles at different values B_r at $t = 0.1$ when, $Pe = 5$, $R_a = 0.3$ and $R_s = 5$.

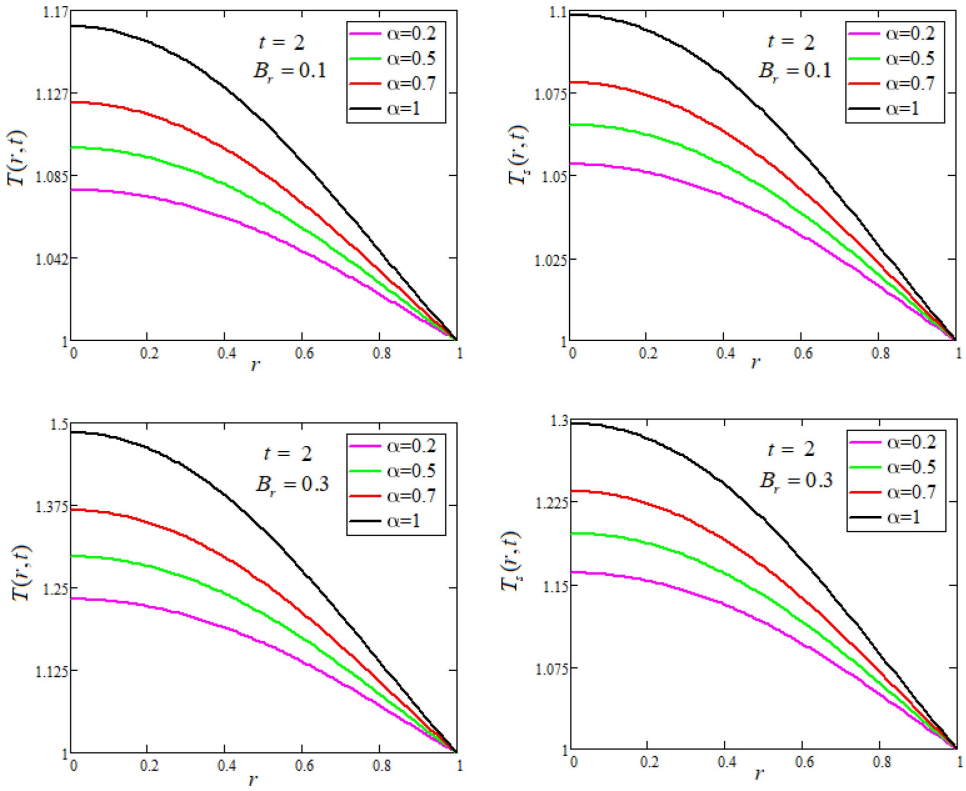

Fig. 14. (Color online) Profiles for temperature of blood and particles at different values B_r at $t = 2$ when $Pe = 5$, $R_a = 0.1$ and $R_s = 5$.

treatment by thermal therapy. Fig. 13, and 14 show the increase in the temperature of blood and particle by increasing the values of B_r. Physically B_r is the ratio of heat generated by viscous forces between the layers of the fluid to the heat transported by the conduction of molecules, so by increasing the values of B_r the heat production by the viscous forces increases due to which the blood and particle temperature increase.

5. Concluding Remarks

- In small & narrow vessels of blood, the non-Newtonian behavior of blood (Casson fluid) is considered with heat conduction between particles and blood.
- In a cylindrical domain, Caputo's fractional time derivative has been taken to examine the impact of different parameters on blood and particles.
- The exact solutions are found by using the Laplace & Hankel transformation jointly.
- The blood and particle velocities increase by increasing the values of Re & β, which is significant in decreasing the blood pressure and in the supply of heat to the tissues of the body and carrying drugs to the affected tissues.
- The blood and particle velocities decrease for increasing the values of H which is useful to control the blood flow during magnetic therapy (for treating pain, such as the back, foot, or joint pain), and surgeries.
- The temperature of blood and particles increase for increasing values of P_e & B_r.
- By increasing the values of R_a decrease the blood and particle temperature. The blood and particle temperature is maximum in the center of the vessel and minimum at the vessel walls, which is significant to avoid affecting the tissues during treatment by thermal therapy.

References

[1] P. A. Voltairas, D. I. Fotiadis, and L. K. Michalis, Journal of Biomechanics **35**, 813 (2002).
[2] W. Andra and H. Nowak, (Eds.) Magnetism in medicine: a handbook (2007) pp 550-567.
[3] J. Plavins and M. Lauva, Journal of Magnetism and Magnetic Materials **122**, 349 (1993).
[4] W. Boyd, Text-book of pathology; structure and function in diseases (1970).
[5] Y. Haik, J. C. Chen, and V. M. Pai, In Proceedings of the IX International Symposium on Transport Properties in Thermal Fluids Engineering, Singapore, Pacific Center of Thermal Fluid Engineering, Hawaii, USA (1996) pp 121-126.
[6] R. K. Dash, K. N. Mehta, and G. Jayaraman, International Journal of Engineering Science **34**, 1145 (1996).
[7] V. P. Rathod and S. Tanveer, Bulletin of the Malaysian Mathematical Sciences Society **32** (2009).
[8] Y. C. Fung, The flow properties of blood. In Biomechanics, Springer, New York (1993) pp 66-108.
[9] D. Sankar, International Journal of Nonlinear Sciences and Numerical Simulation **10**, 1425 (2009).
[10] L. M. Srivastava and V. P. Srivastava, Journal of Biomechanics **17**, 821 (1984).
[11] P. Nagarani, G. Sarojamma, and G. Jayaraman, Acta Mechanica **187**, 189 (2006).
[12] Das, S. Functional fractional calculus, Springer Science & Business Media (2011).
[13] D. S. Sankar and U. Lee, Journal of Mechanical Science and Technology **25**, 2573 (2011).
[14] D. S. Sankar, A. Nagar, and A. V. Kumar, Journal of Applied Fluid Mechanics **8**, 871 (2015).
[15] A. A. Hussien, W. Al-Kouz, M. El Hassan, A. A. Janvekar, and A. J. Chamkha, The European Physical Journal Plus. **136**, 1 (2021).
[16] P. S. Reddy, P. Sreedevi, and A. J. Chamkha, Journal of Thermal Analysis and Calorimetry. 1 (2021).
[17] D. Anderson, J. C. Tannehill, and R. H. Pletcher, Computational Fluidmechanics and Heat Transfer (2016).
[18] L. M. Jiji and L. M. Jiji, Heat convection, Springer-Verlag Berlin Heidelberg (2006).
[19] M. N. Ozisik, Heat conduction, John Wiley & Sons, New York (1993).
[20] N. Khan, F. Ali, M. Arif, Z. Ahmad, A. Aamina, and I. Khan, Mathematical Problems in Engineering (2021).
[21] Z. Ahmad, F. Ali, A. M. Alqahtani, N. Khan, and I. Khan, Fractals, 2240048 (2021).
[22] A. Bhatnagar and R. K. Shrivastav, Int. J. of Innovative Research in Advanced Engineering **1**, 250 (2014).
[23] J. T. Machado, V. Kiryakova, and F. Mainardi, Communications in Nonlinear Science and Numerical Simulation **16**, 1140 (2011).
[24] Z. Ahmad, F. Ali, N. Khan, and I. Khan, Chaos, Solitons & Fractals **153**, 111602 (2020).
[25] S. Murtaza, P. Kumam, Z. Ahmad, T. Seangwattana, and I. E Ali, Fractals (2022).
[26] S. Murtaza, P. Kumam, Z. Ahmad, K. Sittithakerngkiet, and I. E Ali, IEEE Access (2022).
[27] Z. Ahmad, M. Arif, and I. Khan, City University International Journal of Computational Analysis **4**, 18 (2020).
[28] M. Iftikhar, Z. Ahmad, S. Murtaza, I. E Ali, and I. Khan, City University International Journal of Computational Analysis (2022).
[29] N. A. Shah, D. Vieru, and C. Fetecau, Journal of Magnetism and Magnetic Materials **409**, 10 (2016).
[30] M. A. Imran, I. Khan, M. Ahmad, N. A. Shah, and M. Nazar, Journal of Molecular Liquids **229**, 67 (2019).
[31] C. D. K. Bansi, C. B. Tabi, T. G. Motsumi, and A. Mohamadou, Journal of Magnetism and Magnetic Mate-

rials **456**, 38 (2018).
[32] G. W. Sutton and S. Arthur, Engineering Magnetohydrodynamics. (1965).
[33] Copley (ed.), A. L., G. Stainsby, Flow Properties of Blood and Other Biological, Pergamon Press, Oxford, (1960).
[34] N. Casson, Rheology of disperse systems, in Flow Equation for Pigment Oil Suspensions of the Printing Ink Type. Rheology of Disperse Systems (Mill, C. C., ed.), Pergamon Press, London (1959) pp 84-102.
[35] P. Mandal, International Journal of Non-Linear Mechanics **40**, 151 (2005).
[36] S. Sharma, U. Singh, and V. Katiyar, Journal of Magnetism and Magnetic Materials **377**, 395 (2015).
[37] L. Srivastava and V. Srivastava, Journal of Biomechanics **17**, 821 (1984).
[38] N. Ali Shah, D. Vieru, and C. Fetecau, Journal of Magnetism and Magnetic Materials **409**, 10 (2016).
[39] T. Chinyoka and O. D. Makinde, Advances in Mathematical Physics **209**, 231 (2014).
[40] C. B. Tabi, et al. Communications in Nonlinear Science and Numerical Simulation **49**, 1 (2017).
[41] H. A. Attia, A. M. A. Al-Kaisy, and K. M. Ewis, Journal of Applied Science and Engineering **14**, 91 (2011).
[42] E. F. Doungmo Goufo and C. B. Tabi, Chaos: An Interdisciplinary Journal of Nonlinear Science **29**, 023104 (2019).
[43] W. Everitt and H. Kalf, Journal of Computational and Applied Mathematics **208**, 3 (2007).
[44] X. Li, Journal of Mathematical Analysis and Applications **335**, 935 (2007).
[45] S. Das, Functional fractional calculus for system identification and controls, Springer (2008).